Application of associative ionization to the observation of quantum beats in low-lying atomic resonances

J. F. Christian,* L. C. Snoek, S. G. Clement, and W. J. van der Zande†
FOM Institute for Atomic and Molecular Physics, Kruislaan 407, 1098 SJ Amsterdam, The Netherlands
(Received 8 August 1995)

A method is described which allows the detection of atomic quantum beats or wave-packet evolution in low-lying states, phenomena which are usually difficult to observe. The excitation method consists of a phase-sensitive two-pulse technique. Detection of the excited-state population after the two pulses is achieved by monitoring rubidium dimer ions which are formed in the associative ionization reaction, $Rb^*(n)p + Rb \rightarrow Rb_2^+ + e^-$. The dimer ion yield as a function of the wavelength showed strong features, which coincided with the $8p$ to $15p$ atomic resonances. The two-pulse technique revealed atomic fine-structure quantum beats due to the coherent excitation of the $np^2P_{1/2,3/2}$ fine-structure states of the atom.

PACS number(s): 42.50.Md

I. INTRODUCTION

The last 15 years have seen a wealth of time-resolved studies of atomic and molecular motion and molecular reaction dynamics [1–5]. This is not hard to understand, as time-resolved studies often give a more intuitive insight into quantum-mechanical processes. Another aspect is that control over coherence can affect the outcome of chemical reactions [6]. All these techniques have been made possible by the advent of fast (picosecond and femtosecond) tunable laser systems. In many experiments a pump-probe sequence is applied. The first pulse coherently populates a number of eigenstates, while the second pulse interrogates the wave packet created by the first pulse. Here it is essential that the probe pulse is selective in its excitation of the wave packet. For example, if photoionization is used as a probe for (Rydberg) wave-packet evolution, the wave packet is only ionized when it is close to the (atomic) core [2,7]. More recently, two-pulse techniques have been introduced which make use of the coherence, or phase relation, between the two pulses. Fleming and co-workers applied this in molecular physics [8]. They locked the phases of the two pulses and varied the time delay between them. In their experiments the observable was the total excited population after the two-pulse sequence. A variation on this technique for the use in atomic systems has been developed, which does not require the knowledge of the phase difference between the two pulses, but in which the relative phase between them is varied at a known rate [9–11]. The technique, which has strong analogies with Ramsey's separated oscillatory field method [12,13], greatly enhances the detection sensitivity to illustrate dynamics in high-lying Rydberg states. As in Ramsey's method, the population after the two separated excitations has to be determined. The technique has been applied to the study of electron wave-packet motion in highly excited Rydberg states affected by static electric and magnetic fields (e.g., [14–16]). In these experiments field ionization has been used as a means of observing the excited population after the two pulse sequence.

Previous quantum beat spectroscopy experiments of Zeeman splittings in atoms [17] or molecules [18] and of hyperfine and fine-structure intervals [19,20] have been performed by detecting the fluorescence. Other detection methods using, e.g., resonance absorption or stimulated emission have been described in [21,22]. Leuchs and Walther were the first to apply field ionization to observe fine-structure beats in higher n states of sodium [23]. In this paper we present an alternative detection method to probe the population of low-lying excited states, namely applying the associative ionization reaction as ionization mechanism (see, e.g., [24]). This method is applicable in systems where the excitation energies of the (atomic) states of interest are sufficiently high to create an ionized molecule. In the interferometric two-pulse experiment described below, the pump pulse photoexcites a coherent superposition of the $np^2P_{1/2,3/2}$, fine-structure states in atomic rubidium. After a delay, the excitation from the probe pulse interferes either constructively or destructively with that from the pump pulse, depending on the relative phase between them. Constructive interference produces excited rubidium atoms in the $np^2P_{1/2,3/2}$ fine-structure states, destructive interference pumps the population down to the ground state. Subsequent collisions with other rubidium atoms, long after the pump-probe sequence, cause the excited atoms to associatively ionize, thereby producing dimer ions which are an indicator of the excited atomic population. This will occur for levels with $n^* = 7$ and higher. The dimer ion formation is monitored as a function of the time delay between the two pulses, and yields the atomic fine-structure quantum beats. It is of interest to note the following: the pump and probe pulse sequence makes it possible to produce reactants during a very short and well-defined time span [25]. Using an interferometrically stable delay, one can generate excited reactants in time windows of picoseconds, before ionizing or pumping them back to the ground state.

II. THE TWO-PULSE METHOD

This section contains a general description of a two-pulse wave-packet interferometry experiment in which the phase-

*Present address: Department of Physics, Northeastern University, 111 Dana Research Center, Boston, MA 02115.
†Author to whom all correspondence should be addressed.

sensitive detection technique [9,10] is applied. Atomic units are used, unless other units are explicitly indicated.

An atom is exposed to two identical picosecond light pulses from a Michelson interferometer, separated by a time delay τ (see Sec. III). The first pulse creates a wave packet $|\psi_0\rangle$ which has evolved in time to $|\psi_\tau\rangle$ at time τ, when the second pulse arrives. The second pulse creates a wave packet $|\psi_0\rangle$ which is identical to the initial wave packet and can interfere with it. This assumption is only justified if depletion of the ground state by the first pulse can be neglected, which is true in this case, since in the experiment the pulse area is considerably smaller than 0.1π. The similarity between the initial wave packet, after it has evolved for a time τ, and the second wave packet determines the amount of interference between the two. After the two-pulse sequence, the total excited wave function is described by

$$|\Psi_{total}(\tau)\rangle = |\psi_\tau\rangle + |\psi_0\rangle, \tag{1}$$

or, if written in terms of eigenenergies ω_n and amplitudes a_n of the eigenstates $|n\rangle$ of which the wave packets are composed:

$$|\Psi_{total}(\tau)\rangle = \sum_n a_n(1+e^{-i\omega_n\tau})|n\rangle, \tag{2}$$

where we used

$$|\psi_t\rangle = \sum_n a_n e^{-i\omega_n t}|n\rangle, \quad \text{for} \quad t=0,\tau. \tag{3}$$

The excited-state population $P(\tau)$ after the two pulses is given by

$$\begin{aligned} P(\tau) &= \langle\Psi_{total}(\tau)|\Psi_{total}(\tau)\rangle \\ &= \langle\psi_\tau|\psi_\tau\rangle + \langle\psi_0|\psi_0\rangle + 2\,\mathrm{Re}\langle\psi_\tau|\psi_0\rangle \\ &= \sum_n 2|a_n|^2 + 2|a_n|^2\cos(\omega_n\tau). \end{aligned} \tag{4}$$

The first terms in Eq. (4), $\langle\psi_\tau|\psi_\tau\rangle + \langle\psi_0|\psi_0\rangle$ or $\Sigma_n 2|a_n|^2$, respectively, describe the population created incoherently by the two pulses, and are thus independent of time. The other term, $2\,\mathrm{Re}\,\langle\psi_\tau|\psi_0\rangle$ or $\Sigma_n 2|a_n|^2\cos(\omega_n\tau)$, respectively, is a measure of the interference between the two wave packets, and is time dependent. Thus the excited-state population consists of two parts: an incoherent term independent of τ, and a coherent term dependent on τ. Note that $P(\tau)$ oscillates between 0 and $4|a_n|^2$, with an average value of $2|a_n|^2$.

Inherent in this qualitative model developed so far is the assumption that the two light pulses have a well-defined relative phase [8,3]. In the experiment described here, the relative phases of the two pulses are modulated. This has several advantages: the modulation establishes a well-defined phase relationship between the two pulses, and acquisition of the wave-packet signal at the modulation frequency strongly reduces the contribution from other sources. Furthermore, phase modulation allows the observation of the coherent term only, as this is the only phase-dependent part of the signal, and thus the only modulated term. To achieve the phase modulation, an additional time delay $\Delta\tau$ ($\ll\tau$) between the pulse pairs is introduced by "wiggling" a quartz plate in one of the arms of the Michelson interferometer (see Sec. III). The time delay $\Delta\tau$ is on the order of hundreds of femtoseconds, and is therefore a minimal contribution to τ itself, which is on the order of tens of picoseconds. In the experiment we record the square of the time-autocorrelation rather than its absolute value, because it gives a convenient analytic expression. An expression for the experimentally observed signal as a function of the delay time τ can therefore be obtained by squaring the phase modulated part of Eq. (4) and integrating it over the $2\Delta\tau$ time window:

$$\begin{aligned} I(\tau) &= \int_{\tau-\Delta\tau}^{\tau+\Delta\tau} [2\,\mathrm{Re}\langle\psi_{\tau'}|\psi_0\rangle]^2 d\tau' \\ &= \int_{\tau-\Delta\tau}^{\tau+\Delta\tau} \left[\sum_n 2|a_n|^2\cos(\omega_n\tau')\right]^2 d\tau'. \end{aligned} \tag{5}$$

This equation gives a more intuitive picture of the experiment, since it resembles the expression of a collection of n oscillators, each oscillating at their own frequency ω_n, and therefore causing a beating frequency. Extending this idea to two-photon transitions has been recently discussed by Engel and Metiu [3]. The amplitude of an eigenstate in the wave packet, a_n, is determined by the transition moment of the eigenstate, and by the intensity of the laser at that frequency. The eigenenergy, ω_n, is defined with respect to the ground state. Decay and dephasing of the eigenstates can in our case be neglected, considering the conditions in which the experiment is performed (see Sec. IV). The intensity of the wave-packet signal as a function of delay time, $I(\tau)$, is presented in the recurrence spectra given in Sec. IV of this paper.

We would like to note here that, in this experimental method, the beating displayed by $I(\tau)$ does not depend on the species in which the wave packet is created (e.g., pure rubidium or a contaminated sample), but is only determined by the energy spacing in the absorption spectrum, since $I(\tau)$ is the Fourier transform of the absorption spectrum [26]. Therefore in those cases where a spectrum arises from the excitation of different initial states, or even of different atomic or molecular species, the same beating pattern would be observed.

III. EXPERIMENT

In Fig. 1 the schematic of the experiment, which has been described in detail elsewhere [11], is shown. It consists of an optical setup to generate the two-pulse sequences, a vacuum system with an oven to create the rubidium beam, and a quadrupole mass spectrometer to select and detect the ions.

Picosecond, wavelength tunable light pulses, obtained from a cavity-dumped, synchronously pumped dye laser (3.8 MHz, 130 mW, 620−700 nm with Lambdachrome 6501 (DCM Special) dye, 7.5 ps, and a bandwidth of $\approx$ 7 cm $^{-1}$) are frequency doubled in a potassium dihydrogen phosphate (KDP) crystal, producing 2.5-ps pulses with an efficiency of $\approx 1\%$. Each UV pulse is divided into two identical pulses by a Michelson interferometer, and one can be time delayed with respect to the other (time delay τ) using a translation stage in one arm of the interferometer. A wiggling quartz plate in the other arm is used to sweep the precise delay

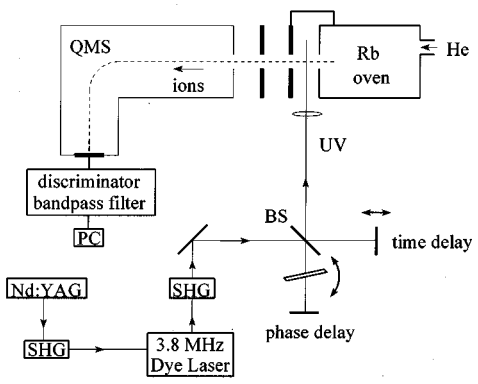

FIG. 1. Experimental setup, consisting of the following components: light source, interferometer, vacuum system and signal acquisition electronics, where SHG denotes second harmonic generator, BS denotes beam splitter, and QMS denotes quadrupole mass spectrometer.

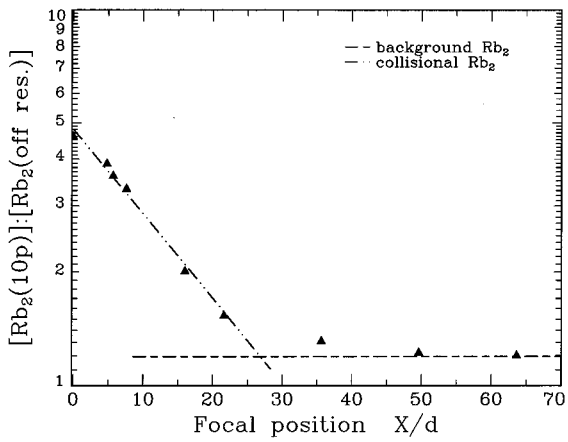

FIG. 2. Ratio between resonant (produced at the wavelength of the atomic $10p$ resonance) and off-resonant (produced by detuning the wavelength of the laser) Rb_2^+ count rates as a function of the distance (X) from the laser focus to the nozzle, measured in nozzle diameters (d). The horizontal line marks the level of background rubidium dimers originating from the source. The other line depicts the quadratic dependence of the collisionally formed dimers on the atomic rubidium density.

($\Delta\tau$) by $\approx$0.4 ps about the ''crude'' delay (τ), thereby sampling $\approx$400 cycles of the optical frequency ν of the laser. This wiggling quartz plate modulates the relative phase of the pulse pair at a rate of 6 kHz, which is slow compared to the repetition rate (3.8 MHz) of the dye laser. The linearly polarized pulses are focused with a 50-cm quartz lens into the vacuum system and the polarization of the light is perpendicular to the molecular beam (see Fig. 1).

In our vacuum chamber, rubidium vapor effuses from the oven through a 0.5-mm-diameter orifice. The rubidium pressure, controlled by an oven temperature of 380 K, is of the order of 4×10^{-4} Torr. At this temperature the equilibrium composition of the vapor contains only 0.02% Rb_2, [27] which accounts for the small dimer background we observe. We sent a small flow of helium at a pressure of $\approx$2 Torr through the oven to prevent the nozzle from clogging.

Ions which are formed after the two pulses in the field-free region between the oven and the first grid, pass a second 95% transmitting grid and are accelerated towards the quadrupole mass spectrometer (Balzers QMG 511, off axis). The resolution of the mass spectrometer was deliberately lowered to collect all isotopomers of the dimer ions ($^{85}Rb_2^+$, $^{87}Rb_2^+$, $^{85,87}Rb_2^+$). A channel electron multiplier connected to a discriminator produces a pulse for each mass selected ion. The mass selected ion signal is sent to a 6-kHz band pass filter, whose frequency matches the modulation frequency of the phase between the two pulses. Therefore only the modulated component of the signal is detected. The intensity variation of the wave-packet signal as a function of delay time τ, is obtained after squaring the output of the filter and averaging it.

IV. RESULTS AND DISCUSSION

While monitoring the Rb_2^+ ion signal as a function of frequency, resonances were observed which coincided with the $5s\rightarrow8p$ through $5s\rightarrow15p$ atomic Rb resonances, superimposed on a small, featureless background that monotonically increased with photon energy. The $n>9np^2P_{1/2,3/2}$ fine-structure states easily fall within the bandwidth of our UV pulses, $\approx$13 cm^{-1}, therefore limiting our observation of fine-structure quantum beats in the time resolved spectra to the $n>9$ states.

The intensity of the dimer ion signal at the atomic resonance, relative to the small off-resonance background, depended strongly upon the distance from the laser focus to the nozzle: the closer to the nozzle, the stronger the resonant contribution to the total dimer ion signal (see Fig. 2). The ratio between the Rb_2^+ count rate at the $10p$ atomic resonance and the off-resonance Rb_2^+ background was measured while varying the distance between the laser focus and the nozzle. In Fig. 2 this ratio is plotted as a function of the focal distance, measured in nozzle diameters. The dimer ion signal results from either the direct photoionization of rubidium dimers in the atomic beam, or from the associative ionization of excited rubidium atoms. The direct photoionization produces a constant background in the ratio of resonant to nonresonant ionization signal, which is illustrated by the horizontal line in Fig. 2. In the high density region near the nozzle associative ionization occurs when a photoexcited rubidium atom collides with a ground-state atom: $Rb^*(n)p+Rb\rightarrow(Rb_2)^*\rightarrow Rb_2^+ + e^-$. This is illustrated by the linear increase in the ratio of the resonant to nonresonant ionization signal near the nozzle in Fig. 2. The excited collision complex, $(Rb_2)^*$, will promptly ionize when its total energy is higher than the ionization potential of the molecule ($V_i=3.45$ eV, with respect to the neutral atoms at infinite separation [28]). This occurs when the Rb^*+Rb system crosses the Rb_2^+ potential-energy curve [29,30], as is the case for our atomic resonances if $n^*\geqslant7$ ($\lambda<359$ nm). The departing electron ''traps'' the system in the Rb_2^+ potential-energy curve. When the mass spectrometer was tuned to the dimer ion mass, ionization from the atomic $8p$ through $15p$ resonances was observed. However, when it was tuned to the atomic rubidium mass, only signals from the $11p$ and higher states were detected. Since the photon energy is too low for direct, one-photon ionization, the atomic signal must

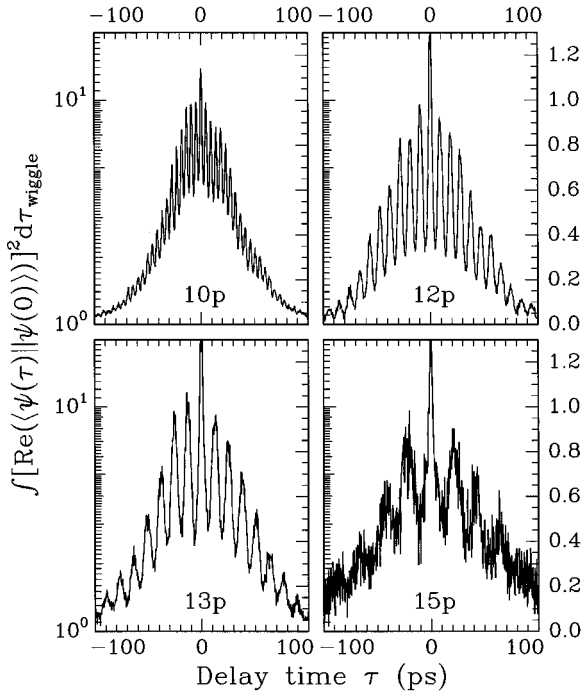

FIG. 3. Dimer ion recurrence spectra: in this figure several atomic np fine-structure quantum beats are presented which have been detected from the Rb_2^+ signal formed via associative ionization. The spacings between the recurrences are determined by the atomic fine-structure splittings: $\tau=2\pi/\Delta\omega$, where $\Delta\omega$ is the energy splitting.

be produced by either two-photon ionization, or by collisional ionization of the excited atomic fine-structure states ($Rb^*+X\rightarrow Rb^+ + e^- + X$, where $X=$Rb or He). At our laser fluence, the contribution of two-photon processes is negligible, and the results of the two-pulse experiment described below will demonstrate that only collisional ionization is responsible for the observed atomic ion signal. No atomic ions originating from the lower n states, $8p$ to $10p$, are observed, since very energetic collisions are required to ionize these states. All collisional processes which produce either Rb_2^+ or Rb^+ occur in the field-free region between the oven and the first grid, well outside the 100-ps window of the two-pulse measurement.

In the two-pulse experiment, coherent superpositions of the $np^2P_{1/2,3/2}$ fine-structure states in the atomic rubidium interfere with each other, either constructively or destructively, depending on the relative phase, thereby enhancing or quenching the ion signal. As has been described in Sec. II, the average amount of the 6-kHz interference is measured in the experiment as a function of the delay time, τ. In Fig. 3, in which the averaged interference is plotted as a function of delay between the pulses, we show some examples of atomic np ($n=10-15$) fine structure quantum beats that were measured with the two-pulse experiment by detecting the dimer-ion mass signal, i.e., the associative ionization signal. The maxima in the spectra are referred to as recurrences, because they indicate when the time-dependent wave function (the wave packet) returns to its initial configuration. These recurrences represent the familiar fine-structure quantum beats, which have been measured by various other techniques as summarized in Ref. [31]. The recurrence times are determined by the atomic fine-structure splittings: $\tau=2\pi/\Delta\omega$, where $\Delta\omega$ is the energy splitting of the fine-structure states. The measured fine-structure splittings recovered by fast Fourier transform from our recurrence spectra for the $10p$ to $15p$ states as presented in Table I, are in good agreement with previously determined values [32]. As has already been mentioned in the last paragraph of Sec. II, the detection method used in this work is not selective for excitation of different initial states or for a contaminated sample. Also the accuracy of the experiment does not allow determination of the hyperfine splitting of the ground state or the isotope shift.

One can see the coherent signal decrease at longer delay times (above 75 ps). This is partly caused by the thermal motion of the atoms, thus by the associated Doppler width, giving the envelope of the spectra a Gaussian appearance. In ''phase language'' one would say that if, between the pump and the probe pulse, the atom moves over a significant fraction of the wavelength of the incident light, it will observe the probe pulse to have a slightly different phase than the pump pulse, and a decrease in the coherent signal will occur. Other sources of dephasing (happening within the 100-ps time window of the delay scan), e.g., caused by collisions in the beam, can be disregarded in view of the low pressures present in the interaction chamber. Another source of dephasing can arise from imperfections in the delay line of the Michelson interferometer. This causes the two pulses to follow the same beam path only when they are temporally overlapped (at $\tau=0$), and leads to a reduced phase modulated signal at $\tau>0$. The envelope of the spectra is called ''the instrument function,'' and can be determined experimentally from the recurrence spectrum of a single eigenstate, e.g., of the $8p$ state, of which the fine-structure splitting is larger than the laser bandwidth. To observe these lower np fine-structure recurrences ($n=7-9$), subpicosecond pulses (larger bandwidth) are needed. The measured recurrence spectra were not background free, since the Gaussian profile was superimposed upon a constant offset for each spectrum. Therefore the 6-kHz contribution from sources other than the

TABLE I. Fine-structure splittings of the $^2P_{1/2,3/2}$ levels in atomic rubidium measured by detection of the associative ionization reaction products (Rb_2^+) and collisional ionization products (Rb^+), compared with the values from Ref. [32].

	$10p$	$11p$	$12p$	$13p$	$14p$	$15p$
This work, Rb_2^+ (cm^{-1})	7.25(4)	4.95(3)	3.52(3)	2.60(2)	1.98(3)	1.52(3)
Rb^+ (cm^{-1})		4.96(2)	3.52(2)	2.60(2)	1.98(2)	1.51(8)
Moore [32] (cm^{-1})	7.31	4.97	3.54	2.60	2.00	1.53

modulated quantum beat signal had to be subtracted out, before the spectra could be normalized. The normalization can be done at $\tau=0$, since there $|\langle\psi(0)|\psi(\tau)\rangle|\equiv 1$. The zero intensity level has been chosen to be at long delays where the signal has completely dephased, the top of the envelope has been defined as the maximum intensity level (unity), disregarding higher intensities at $\tau=0$. At zero delay, the dimer recurrence spectra in Fig. 3 reveal a small, but distinct spike, which is produced by direct photoionization of the dimers originating from the oven and the expansion. At $\tau=0$ the pump and probe pulses coincide, and the wiggling of the phase delay continuously switches the UV on and off. Therefore all laser dependent signals are modulated at 6 kHz at $\tau=0$ and will contribute to the height of the zero-delay peak.

The modulation depth of the recurrences in the spectrum indicates the relative population of the contributing states. Considering the bandwidth of our ps UV pulses, ≈ 13 cm^{-1}, we assume that we equally excite both fine-structure states ($n>9$, $\Delta\omega<7$ cm^{-1}). Excess amplitude from the $^2P_{3/2}$ state produces a delay independent background in the two-pulse experiment. The observed beating is between the amplitude of the $^2P_{1/2}$ state, and the equal amplitude of the $^2P_{3/2}$ state. The measured intensity in the experiment directly reflects the eigenstate amplitudes (squared), which are determined by the transition probabilities for exciting the particular eigenstates in the wavepacket. Indeed in all recurrence spectra the well known intensity ratio 2:1 of the doublet terms $^2P_{3/2}$ and $^2P_{1/2}$ can be recognized in the modulation depths of the spectra, especially at the shorter delay times (up to 50 ps).

For comparison some of the $n=11-15$ recurrence spectra obtained from measuring the atomic ion signal are shown in Fig. 4, where exactly the same fine-structure beatings can be recognized as in the dimer spectra. Compare, in particular, the height of the peaks at zero delay in these spectra with the dimer spectra of Fig. 3. If the production of atomic ions was caused by resonant two-photon ionization, there would have been an increased zero-delay peak in the spectra of Fig. 4, similar to those seen in Fig. 3 for the dimers. The absence of this increased spike in Fig. 4 leads us to the conclusion that the atomic ions are only produced by collisional ionization of the excited atoms. That also explains why no atomic ion signal originating from the lower n states, $8p$ to $10p$, was observed in the frequency scans, since only very energetic collisions can ionise these states. Notice that the ratio of the quantum beats to the background is roughly constant in both Figs. 3 and 4, reflecting the transition probabilities of the atomic fine-structure levels.

No structure in the dimer recurrence spectra was observed when the laser was detuned from an atomic resonance. The fact that dimers do not give rise to observable recurrences in this experiment, is probably caused by the high density of states which is excited in the relatively hot rubidium dimers. Although this is unfortunate if one is interested in observing wavepacket motion in rubidium dimer molecules, it facilitates the interpretation of the dimer spectra taken at the atomic resonances, since all recurrent structure is now due to the fine-structure beats in the atom.

The evolution of the fine-structure wave packets shown in this work illustrate the peculiar nature of electron spin. The most classical analogy of the ''motion'' associated with the fine-structure wave packet is that of a particle, the electron, whose spin axis is precessing in time around the angular momentum vector as it orbits the nucleus. One should, however, pay attention to the fact that, unlike in (Rydberg) electron wave packets, a fine-structure wave packet does not localize the orbital motion of the electron, since only one n state is excited and therefore a stationary n state has been created. It should rather be seen as a kind of alignment effect which is detected: if the orientation of the electron spin created by the second (linearly polarized) pulse is the same as the evolved one created by the first pulse, a maximum in intensity is observed.

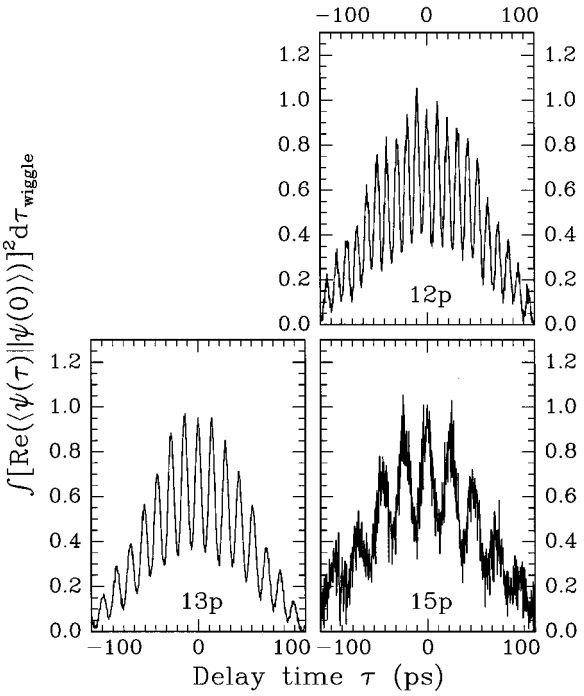

FIG. 4. Atomic ion recurrence spectra: for comparison we show here some recurrence spectra obtained from the collisional ionization of photoexcited atomic Rb, where the same fine-structure beatings can be recognized as in the dimer recurrence spectra. Note the relative height of the peaks around zero delay compared to those in Fig. 3.

V. CONCLUSIONS

The application of associative ionization as a means of measuring the excited-state population arising from an interferometric two pulse wave-packet experiment of low lying atomic resonances has been demonstrated. This method enables us to study those states which are otherwise hard to observe with detection methods such as field ionization. The measured fine structure splittings are in good agreement with literature values.

ACKNOWLEDGMENTS

The authors would like to thank Dr. B. Broers, Dr. C. Snoek, Dr. L.D. Noordam, Professor H.B. van Linden van

den Heuvell, and Professor H.G. Muller for their interest in our work, which was shown in many stimulating and instructive discussions. This work is part of the research program of the Stichting voor Fundamenteel Onderzoek der Materie (Foundation for Fundamental Research on Matter) and was made possible by financial support from the Nederlandse Organisatie voor Wetenschappelijk Onderzoek (Dutch Organisation for the Advancement of Research).

[1] G. Alber, H. Ritsch, and P. Zoller, Phys. Rev. A **34**, 1058 (1986).
[2] A. ten Wolde, L.D. Noordam, A. Lagendijk, and H.B. van Linden van den Heuvell, Phys. Rev. Lett. **61**, 2099 (1988).
[3] V. Engel and H. Metiu, J. Chem. Phys. **100**, 5448 (1994).
[4] M. Nauenberg, C. Stroud, and J. Yeazell, Sci. Am. **270**, 24 (1994).
[5] A.H. Zewail, *Femtochemistry: Ultrafast Dynamics of the Chemical Bond* (World Scientific, Singapore, 1994).
[6] P. Brumer and M. Shapiro, in *Coherence Phenomena in Atoms and Molecules in Laser Fields*, edited by A.D. Bandrauk and S.C. Wallace (Plenum Press, New York, 1992), p. 291.
[7] J.A. Yeazell, M. Mallalieu, and C.R. Stroud, Jr., Phys. Rev. Lett. **64**, 2007 (1990).
[8] N.F. Scherer, A.J. Ruggiero, M. Du, and G.R. Fleming, J. Chem. Phys. **93**, 856 (1990).
[9] L.D. Noordam, D.I. Duncan, and T.F. Gallagher, Phys. Rev. A **45**, 4734 (1992).
[10] B. Broers, J.F. Christian, J.H. Hoogenraad, W.J. van der Zande, and H.B. van Linden van den Heuvell, Phys. Rev. Lett. **71**, 344 (1993).
[11] J.F. Christian, B. Broers, J.H. Hoogenraad, W.J. van der Zande, and L.D. Noordam, Opt. Commun. **103**, 79 (1993).
[12] N.F. Ramsey, Phys. Rev. **78**, 695 (1950).
[13] N.F. Ramsey, *Molecular Beams* (Oxford University Press, Oxford, 1956), p. 122, and references therein.
[14] B. Broers, J.F. Christian, and H.B. van Linden van den Heuvell, Phys. Rev. A **49**, 2498 (1994).
[15] J. Wals, H.H. Fielding, J.F. Christian, L.C. Snoek, W.J. van der Zande, and H.B. van Linden van den Heuvell, Phys. Rev. Lett. **72**, 3783 (1994).
[16] G. Raithel, H. Held, L. Marmet, and H. Walther, J. Phys. B **27**, 2849 (1994).
[17] W. Gornik, D. Kaiser, W. Lange, J. Luther, and H.H. Schultz, Opt. Commun. **6**, 327 (1972).
[18] R. Wallenstein, J.A. Paisner, and A.L. Schwalow, Phys. Rev. Lett. **32**, 1333 (1974).
[19] S. Haroche, J.A. Paisner, and A.L. Schwalow, Phys. Rev. Lett. **30**, 948 (1973).
[20] S. Haroche, M. Gross, and M.P. Silverman, Phys. Rev. Lett. **33**, 1063 (1974).
[21] T.W. Ducas, M.G. Littman, and M.L. Zimmermann, Phys. Rev. Lett. **35**, 1752 (1975).
[22] W. Lange and J. Mlynek, Phys. Rev. Lett. **40**, 1373 (1978).
[23] G. Leuchs and H. Walther, Z. Phys. A **293**, 93 (1979).
[24] Y. Lee and B.H. Mahan, J. Chem. Phys. **42**, 2893 (1965).
[25] V. Blanchet, M.A. Bouchene, O. Cabrol, and B. Girard, Chem. Phys. Lett. **233**, 491 (1995).
[26] G.M. Lankhuijzen and L.D. Noordam, Phys. Rev. A **52**, 2016 (1995).
[27] A.N. Nesmeyanov, *Vapor Pressure of the Chemical Elements* (Elsevier Publishing Company, Amsterdam, 1963).
[28] A.A. Radzig and B.M. Smirnov, *Reference Data on Atoms, Molecules, and Ions* (Springer-Verlag, Berlin, 1985).
[29] A. Valance, J. Chem. Phys. **69**, 355 (1978).
[30] H. Suemitsu, H. Kitaura, R. Yokoyama, M. Ehara, and H. Nakatsuji, J. Phys. B **25**, 4507 (1992).
[31] T.F. Gallagher, in *Rydberg Atoms*, 1st ed. (Cambridge University Press, Cambridge, 1994), p. 355.
[32] C.E. Moore, *Atomic Energy Levels* (U.S. Department of Commerce, Washington D.C., 1952).